Weld Heat-Affected Zone in Ti-6Al-4V Alloy, Part I — Computer Simulation of the Effect of Weld Variables on the Thermal Cycles in the HAZ

Computer simulation is a useful tool for visualizing the interrelationships of various weld variables and their effects on thermal cycles

BY A. K. SHAH, S. D. KULKARNI, V. GOPINATHAN AND R. KRISHNAN

ABSTRACT. The weld thermal cycles encountered in the HAZ of titanium alloys have been characterized using modified Rosenthal equations. The results are shown in the form of axonometric plots depicting the effect of two weld variables keeping the other variables fixed. Computer simulation results show that the heat input and the plate thickness are the major variables affecting the thermal cycles in the HAZ. The effects of changes in welding speed are reflected in the variation in the heat input. The electrode radius has minimal effect and can be termed as the minor variable. Preheat or interpass temperatures have an intermediate effect. An increase in electrode radius or decrease in plate thickness requires large apparent displacement of the heat source above the plate surface to be incorporated in the analytical solutions. The melt pool width increases sharply with an increase in the heat input (q/v) or a decrease in plate thickness (d); however, preheat temperature (T_0) has negligible effect. The effect of weld variables on the effective heat input is also similar. The $t_{8/5}$ parameter increases sharply with reducing plate thickness or increasing heat input.

A. K. SHAH is with Naval Chemical and Metallurgical Laboratory, Naval Dockyard, Bombay, India. S. D. KULKARNI and V. GOPINATHAN are with Dept. of Metallurgical Engineering, Indian Institute of Technology, Bombay, and R. KRISHNAN is with Gas Turbine Research Establishment, Bangalore, India.

Introduction

Welding is one of the fastest and most reliable manufacturing processes used for critical applications. Good inherent weldability is a characteristic that is highly desirable in an alloy intended for structural applications. Even in components not intended to be manufactured by welding, weldability is an important consideration in material selection because it provides an option for repairing improperly machined or defective parts as well as repairing in-service damage.

The weldability of a material is not simply a material property but is affected by the design, the welding parameters, and numerous other factors (Ref. 1). The mechanical properties of a welded material depend on the microstructure, which, in turn, depends on the transformation characteristics as governed by the continuous-cooling-transformation (CCT) diagrams. The transformation characteristics are controlled by the heating and cooling process, *i.e.*, the temperature-time cycle at every point of the weldment. The temperature-time cycles are determined by the welding conditions (heat input, preheat/interpass temperature, plate thickness, welding process and joint geometry) and the physical properties (thermal conductivity, specific heat, etc.) of the material being welded. Hence, it is necessary to study the effect of weld variables on the thermal cycles in the HAZ in order to optimize the properties of the weldment. This information can be used for selection of the weld variables to be used for a particular application.

KEY WORDS

Ti-6Al-4V Alloy
Heat-Affected Zone
Computer Simulation
Weld Thermal Cycles
Weld Variables
Rosenthal Equations
Heat Input
Plate Thickness
Preheat Temperature
Interpass Temperature

Titanium and its alloys find applications because of their excellent corrosion resistance and high specific strength properties, however, a major hindrance in the growth of titanium usage has been the potential for degradation of mechanical properties, *e.g.*, ductility, as a result of welding, in many of the newly developed high-strength alloys.

The present work was undertaken to study the effect of weld variables on the thermal cycles in the HAZ in the case of titanium welding. The analytical heat flow equations of Rosenthal have been appropriately modified so that the errors due to the various assumptions are minimized. The results presented in the form of axonometric plots can be used to visualize the effect of various weld variables and help select the optimum vari-

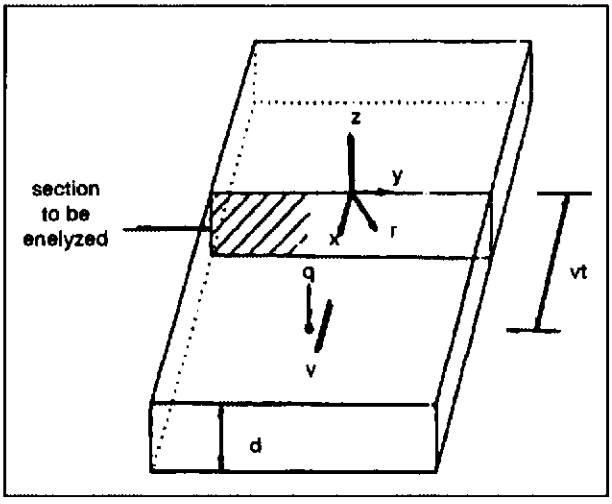

Fig. 1 — Welding configuration showing the coordinate system for heat flow analysis.

ables for a particular application.

Mathematical Modeling

The first efforts in quantifying weld thermal cycles were started in the early 1940s (Ref. 2). As a result of quantitative temperature measurements in the heat-affected zone of arc welds, a series of differential equations was developed (Refs. 3, 4) expressing the temperature distribution in the neighborhood of an electric arc weld as a function of time, distance from weld centerline, and welding variables. The analytical solution to the heat flow problem in welding was derived by Rosenthal (Ref. 5) and was later reviewed by other investigators (Ref. 6). The limitations of the simplifying assumptions in the earlier efforts have consequently led to attempts by many others (Refs. 7–18) to suitably modify the analytical solutions to account for the various assumptions. However, due to the complex nature of the heat flow problem, the modified analytical solutions, or even computer simulated models, so far have had rather limited success in characterizing the thermal cycles in the weld pool (Refs. 19, 20). But in the HAZ region, even the modified analytical solutions are able to characterize the thermal cycles with adequate accuracy for practical purposes (Refs. 19–21).

Rosenthal (Ref. 5) applied the exact theory of heat flow due to a moving source to arc welding situations. The various assumptions made by Rosenthal are:

1) A moving point/line source represents the weld arc.

2) Material properties are unaffected by changes in temperature.

3) Heat losses at the plate surface due to convection are negligible.

4) The latent heat change due to phase transformations is negligible.

Application of the heat flow equations to the thermal cycles experienced by the HAZ (assuming instantaneous application of heat) at a certain fixed position from the heat source as defined by a radial distance r (Fig. 1), gives, for thick plates:

$$T - T_o = \left\{\frac{q/v}{2\pi\lambda t}\right\} exp\left\{\frac{-r^2}{4at}\right\} \quad (1)$$

and for thin plates

$$T - T_o = \frac{q/v}{d(4\pi\lambda\rho c\, t)^{\frac{1}{2}}}\ exp\left\{\frac{-r^2}{4at}\right\} \quad (2)$$

where, t= time (s); λ = thermal conductivity (J/m s K); a = thermal diffusivity = λ/ρc (m^2/s); r = radial distance, m; T = temperature K; T_o = initial temperature = preheat/interpass temperature (K); ρc = specific heat per unit volume (J/m^3 K); ρ = mass density (kg/m^3); c = specific heat at constant pressure (J/kgK); q/v = heat input (KJ/m); q = V·I = arc power (W); V = arc voltage (V); I = welding current (A); v = arc velocity (m/s); d = plate thickness (m).

These are first-order solutions of the differential equations and are applicable only at temperatures outside the fusion zone (Ref. 5), *i.e.*, HAZ.

Table 1 — Typical Welding Parameters for Titanium Welding Reported in the Literature

Welding Process	r_B (mm)	v (mm/s)	Plate Thickness (mm)	Heat Input (kJ/mm)	d_{crit} (mm)	Type of Heat Flow	$t_{8/5}$ s	Ref.
GTAW	1.6	4.0	12.5	1.1	19.79	2D	14.1	29
GTAW	1.6	4.0	12.5	1.2	20.64	2D	16.7	28
GTAW	0.8	3.39	1.0	0.11	6.14	2D	20.4	23
GTAW	1.6	4.5	6.4	0.95	18.11	2D	37.6	25
GTAW	0.8	2.54	0.6	0.12	6.01	2D	52.0	25
GTAW	1.6	3.39	12.7	2.4	28.83	2D	61.3	26
GTAW	1.6	3.39	12.5	2.4	28.81	2D	63.1	28
GTAW	1.2	3.39	3.2	0.74	15.22	2D	75.0	27
GTAW	0.8	3.39	2.5	0.7	14.16	2D	92.3	30
GTAW	1.2	3.39	2.0	0.64	13.47	2D	117.9	23
GTAW	1.6	2.54	12.5	3.96	36.41	2D	161.1	27
GTAW	0.6	2.30	4.5	1.8	22.77	2D	190.3	24
GTAW	1.2	2.12	2.3	1.10	16.70	2D	210.8	23
GTAW	1.6	3.39	6.25	2.66	28.51	2D	242.4	27

In case values are not specified normal values are taken.

Selection of Heat Flow Model for Titanium Welding

The choice of the equation to be used for a particular case is governed not only by the plate thickness and weld parameters but by the weld process and even the type of material. The values of weld parameters and the calculated critical thickness, d_{crit}, which defines the crossover or boundary condition between two-dimensional and three-dimensional heat flow (Ref. 22) are listed in Table 1. It is seen from literature data (Refs. 23–30) that, in the case of titanium, the heat flow is two dimensional for most practical welding conditions. Hence, for further modelling, only two-dimensional heat flow has been considered.

From experimental measurements of the weld thermal cycle, it has been found that for a given welding process, weld geometry, and material properties, the cooling time, $t_{8/5}$, through the range 800°–500°C (1073–773 K) is constant, at least within the HAZ (Ref. 1): $q/v \propto t_{8/5}$ = constant.

These analytical solutions can be expressed in terms of T_p, $t_{8/5}$ and T_o. The solution for thin plates is

$$T_p - T_o = \left\{\frac{2}{\pi e}\right\}^{\frac{1}{2}}\left\{\frac{q/v}{2d\ \rho c r}\right\} \quad (3)$$

$$\theta_2 = \left\{\frac{1}{773 - T_o}\right\}^2 - \left\{\frac{1}{1073 - T_o}\right\}^2 \quad (4)$$

$$t_{8/5} = \left\{\left\{\frac{q}{vd}\right\}^2 \frac{1}{4\pi\lambda\rho c}\right\}\theta_2 \quad (5)$$

$$T - T_o = \left\{\frac{t_{8/5}}{t \cdot \theta_2}\right\}^{\frac{1}{2}} exp\left\{\frac{t_{8/5}}{2et \cdot \theta_2 (T_p - T_o)^2}\right\} \quad (6)$$

where, T_p = peak temperature.

In the above equations, it is assumed that the total heat generated in the arc is transferred to the weld metal. But, practically, only part of the heat input (q/v =

Table 2 — Welding Parameter Data Used for Computer Simulation

Welding speed, v	3–6 mm/s
Electrode radius, r_B	0.6, 0.8 and 1.2 mm
Plate thickness, d	0.5–13.0 mm
Heat Input, q/v	0.1–4.0 kJ/mm
Preheat temperature, T_o	25–125°C
$t_{8/5}$ parameter	1–250 sec
Peak temperature	650–1650°C
Thermal efficiency, η	0.8 (Ref. 33)

Table 3 — Material Property Data for Ti-6Al-4V Alloy

Parameter	Value	Ref.
Thermal conductivity, λ	20.0 J/msK	34,35
Volume thermal capacity, ρc	3.75×10^6 J/m³K	34,36
Melting point, T_m	1933 K	34
Latent heat of melting per unit volume, L	1.95×10^9 J/m³	37

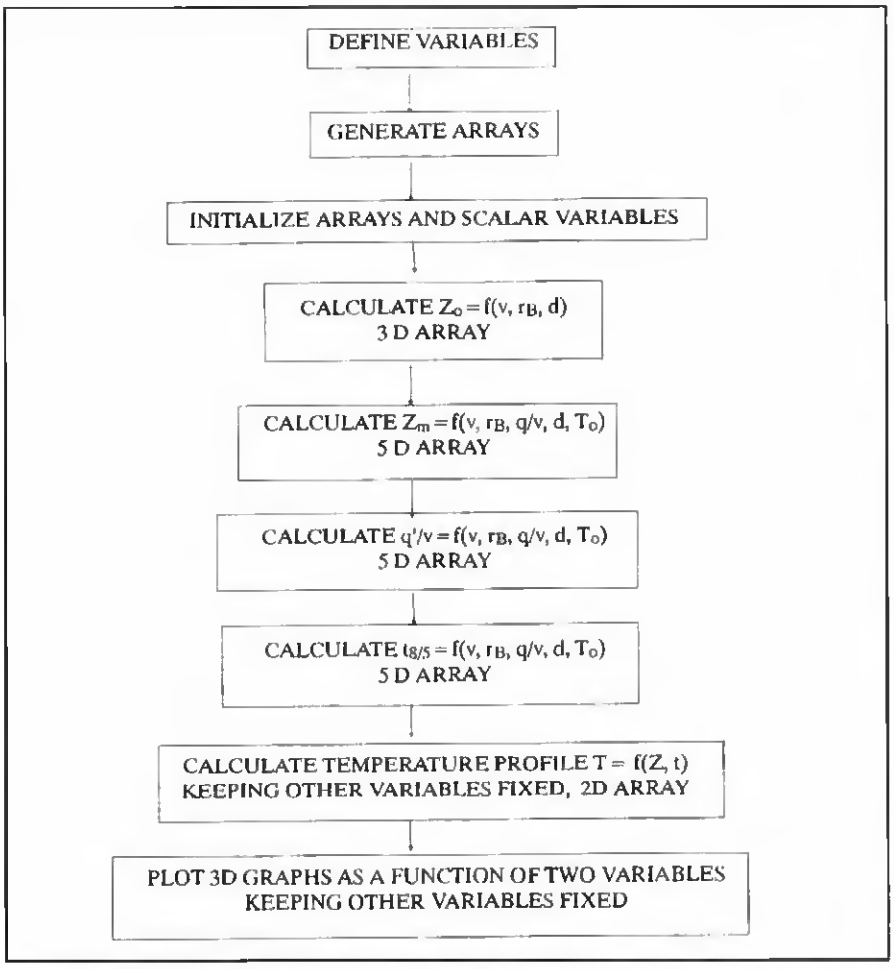

Fig. 2 — Flowchart for the evaluation of effect of weld variables on the weld thermal cycles.

V.I/v) calculated on the basis of welding parameters is transferred to the base metal since a part of the heat is lost to the surroundings by radiation or by conduction through the torch nozzle. This can be accounted for by multiplying the heat input by the arc efficiency factor (η). In this paper the GTAW process is modeled since it is most commonly employed for welding titanium and its alloys. However, the model could be extended to other processes with suitable modifications.

The results of a study (Ref. 13) conducted to find the effect of joint geometry on the cooling time $t_{8/5}$ as compared to the bead-on-plate test show that the cooling time $t_{8/5}$ for fillet welds is less compared to the cooling time for bead-on-plate tests for the same welding conditions. It is also seen that $t_{8/5}$ depends on plate thickness, heat input, and sequence number of the pass, for T or X joints. Hence, to account for these effects of joint geometry on the cooling cycle, a correction factor, F_2, termed as notch factor has to be introduced in the $t_{8/5}$ relations. Thus, the relation for $t_{8/5}$ for two-dimensional heat flow becomes :

$$t_{8/5} = \left\{\left(\frac{\eta q}{vd}\right)^2 \frac{1}{4\pi\lambda\rho c}\right\} \left\{\left(\frac{1}{773-T_o}\right)^2 - \left(\frac{1}{1073-T_o}\right)^2\right\} \cdot F_2 \qquad (7)$$

Modeling of Temperature Profile by Finite Source Model

In the far heat-affected zone, the Rosenthal (Ref. 5) equations provide a good approximation of the thermal cycles. However, both the point (Ref. 5) and line (Refs. 6, 7) source models lead to infinite temperatures at the surface where the arc impinges. Hence, they are less satisfactory in describing the physical shape of the melt pool or the neighboring near HAZ isotherms. The use of the "finite source" model can lead to better approximations in the near HAZ.

Considering a cylindrical arc of radius r_B delivering a power density q_s (x, y) such that the total power in the arc is:

$$q = \int_0^\infty \int_0^\infty q_s \, dx \, dy \qquad (8)$$

for the case of a Gaussian power density:

$$q_s = q_{max} \cdot exp\left\{-\left\{\frac{x^2+y^2}{r_B^2}\right\}\right\} \qquad (9)$$

where r_B is the distance from the arc center at which the power density has fallen to 1/e of its peak value q_{max}. In the present study, it is assumed that r_B is proportional to the radius of the welding electrode.

The temperature field produced by a point heat source for two-dimensional heat flow (thin plates), in the HAZ (assuming instantaneous application of heat) at a certain fixed position from the heat source is given by Equation 2. However, a diffuse arc with Gaussian energy distribution tracking in the x direction with velocity, v, can be treated as a line source of finite width in the y direction but infinitesimally thin in the x direction, if the velocity, v, of the arc is high. The analytical solution for the temperature field T (y, z, t) is given by:

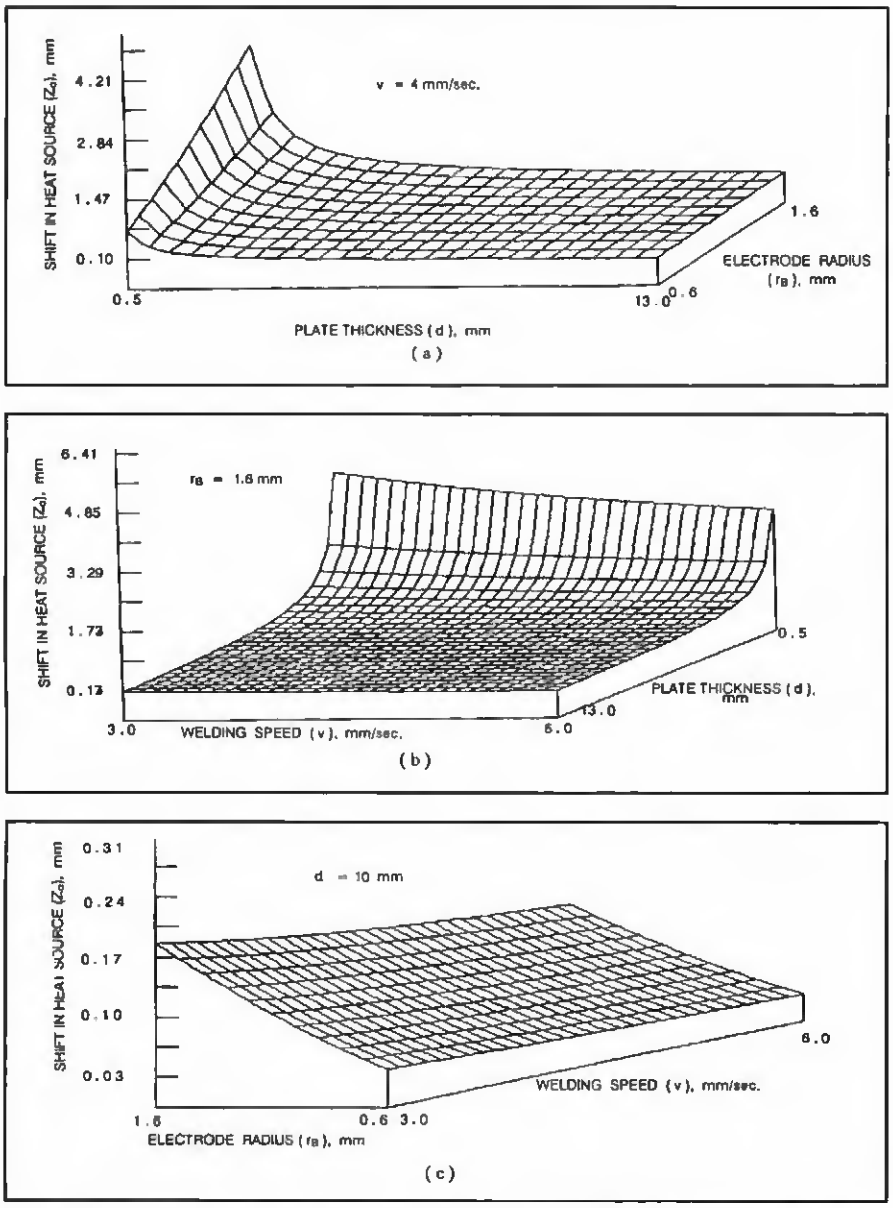

Fig. 3 — Shift in heat source above the plate surface as a function of weld variables. A — r_B and d; B — v and d; C — r_B and v.

$$T - T_o = \frac{q/v}{d\sqrt{4\pi\lambda\rho c}} \cdot \left\{\frac{1}{t(t+t_o)}\right\}^{\frac{1}{4}} \cdot exp\left\{\frac{-1}{4a}\left\{\frac{Z^2}{t} + \frac{y^2}{t+t_o}\right\}\right\}$$

$$\text{where } t_o = \frac{r_B^2}{4a} \tag{10}$$

t_o is the time taken for the heat to diffuse over the arc half width r_B. Far from the heat source where $Z^2 + y^2 >> q/rB^2$ and $t >> t_o$, this is equivalent to the point heat source solution, Equation 2. This equation also leads to infinite temperatures at the surface where the arc impinges. This is because of the assumption of instantaneous application of energy at time t = 0. To overcome this, the width of the arc in both x and y directions should be taken.

Displacement of Finite Source

Using the model of Ashby and Easterling (Ref. 31), it can be described as follows. If the arc has a radius of r_B, then the energy is injected at a given point on the surface over a time, t_B :

$$t_B = C_1\left\{\frac{r_B}{v}\right\} \tag{11}$$

Where C1 is a constant near unity. Hence heat diffuses inward during the injection time, draining heat away from the surface, thereby limiting the surface temperature to a finite value. This can be incorporated by replacing the real source in the plane Z = 0 by an apparent source in the plane $Z = Z_0$ above the surface, so that Equation 10 reduces to:

$$T - T_o = \frac{q/v}{d\sqrt{4\pi\lambda\rho c}} \cdot \left\{\frac{1}{t(t+t_o)}\right\}^{\frac{1}{4}} \cdot exp\left\{\frac{-1}{4a}\left\{\frac{(Z+Z_o)^2}{t} + \frac{y^2}{t+t_o}\right\}\right\} \tag{12}$$

Just below the arc, *i.e.*, y = 0, we get:

$$T - T_o = \frac{q/v}{d\sqrt{4\pi\lambda\rho c}} \cdot \left\{\frac{1}{t(t+t_o)}\right\}^{\frac{1}{4}} \cdot exp\left\{-\left(\frac{Z+Z_o}{at}\right)^2\right\} \tag{13}$$

In the case of far HAZ, *i.e.*, $r >> r_B$, this reduces to the Rosenthal solution, Equation 2. Differentiating Equation 13, w.r.t time (t) will give the heating and cooling rates:

$$\frac{dT}{dt} = \frac{T - T_o}{4t}\left\{\frac{(Z+Z_o)^2}{at} - \frac{2t+t_o}{t+t_o}\right\} \tag{14}$$

The first term pertains to heating and the second to cooling. The peak temperature of the thermal cycle can be obtained by equating dT/dt = 0 in Equation 14. Hence at peak temperature, T_p :

$$\frac{(Z+Z_o)^2}{a} = \frac{t(2t+t_o)}{t+t_o} \tag{15}$$

The value of Z_0 can be evaluated from Equation 15 by considering the cases of time $t >> t_o$ and $t << t_o$. Considering the time scale encountered in welding processes, it is reasonable to assume that $t >> t_o$. Hence, Equation 15 can be simplified to:

$$t = \frac{(Z+Z_o)^2}{2a} \tag{16}$$

Now solving Equations 16 and 13 we get the peak temperature T_p as:

$$T_p - T_o = \left\{\frac{2}{\pi e}\right\}^{\frac{1}{2}} \frac{q/v}{2d\rho c(Z+Z_o)} \tag{17}$$

This reduces to the Rosenthal's point source solution, Equation 3, when $Z >> Z_0$. From Equation 17, the depth at which a particular T_p is reached can be obtained as:

$$Z + Z_o = \left\{\frac{2}{\pi e}\right\}^{\frac{1}{2}} \frac{q/v}{2d\rho c(T_p - T_o)} \tag{18}$$

The value of Z_0 can be determined by using the solution of Bass (Ref. 32), for the peak surface temperature (T_s) produced by a stationary arc of intensity q/r_B^2, applied for a time t_B, *i.e.*:

$$T_s - T_o = \left\{ \frac{2q}{\lambda \pi^{\frac{3}{2}} r_B^2} \right\} \{ a t_B \}^{\frac{1}{2}} \tag{19}$$

Equating with Equation 17 for Z = 0 we get:

$$Z_o = \left\{ \frac{\pi r_B}{2d} \right\} \left\{ \frac{a t_B}{2ev} \right\}^{\frac{1}{2}} \tag{20}$$

Latent Heat Correction

When the melt pool is formed, energy is absorbed as latent heat of melting. Although this energy is released later, it is temporarily removed from the input energy and is stored in the melt pool, and thus, this amount of energy is not available to melt more material. Hence, a point in a solid metal experiences a heat input which is reduced by this amount. If the melt pool is approximated by a half-cylinder of radius Z_m, then the volume that melts per second is $\pi Z^2_m v/2$ and the effective energy input q' is:

$$q' = q - \frac{\pi Z_m^2 v L}{2} \tag{21}$$

where L is the latent heat of melting per unit volume. The melt pool depth Z_m can be calculated by substituting $T_p = T_m$, $Z = Z_m$ and q = q' in Equation 18 and solving the resultant quadratic equation for Z_m, *i.e.*:

$$A_1 Z_m^2 + Z_m + (Z_o - A_2) = 0$$

$$\text{where } A_1 = A_0 \frac{\pi L}{2},\ A_2 = A_0 \cdot q/v,$$

$$A_0 = \left\{ \frac{2}{\pi e} \right\}^{\frac{1}{2}} \left\{ \frac{1}{2d\rho c\,(T_m - T_o)} \right\} \tag{22}$$

where, substituting the value of Z_m in Equation 21, we get the value of q' used for subsequent calculations.

The time constant $t_{8/5}$, *i.e.*, the cooling time from 800° to 500°C (1073–773 K), can be obtained from Equation 13, for the case $t >> t_o$, and it is same as Equation 7.

The temperature profile of Equation 13 can now be represented in terms of $t_{8/5}$ and T_p, as:

$$t_{8/5} = \left\{ \frac{q'}{vd} \right\}^2 \frac{\theta_2}{4\pi\lambda\rho c} F_2 \tag{23}$$

$$T_p - T_o = \left\{ \frac{2}{\pi e} \right\}^{\frac{1}{2}} \frac{q'/v}{2d\rho c(Z - Z_o)} \tag{24}$$

$$T - T_o = \left\{ \frac{t_{8/5}}{\theta_2} \right\}^{\frac{1}{2}} \left\{ \frac{1}{t(t + t_o)} \right\}^{\frac{1}{4}} \exp - \left\{ \frac{t_{8/5}}{2et\theta_2 (T_p - T_o)^2} \right\} \tag{25}$$

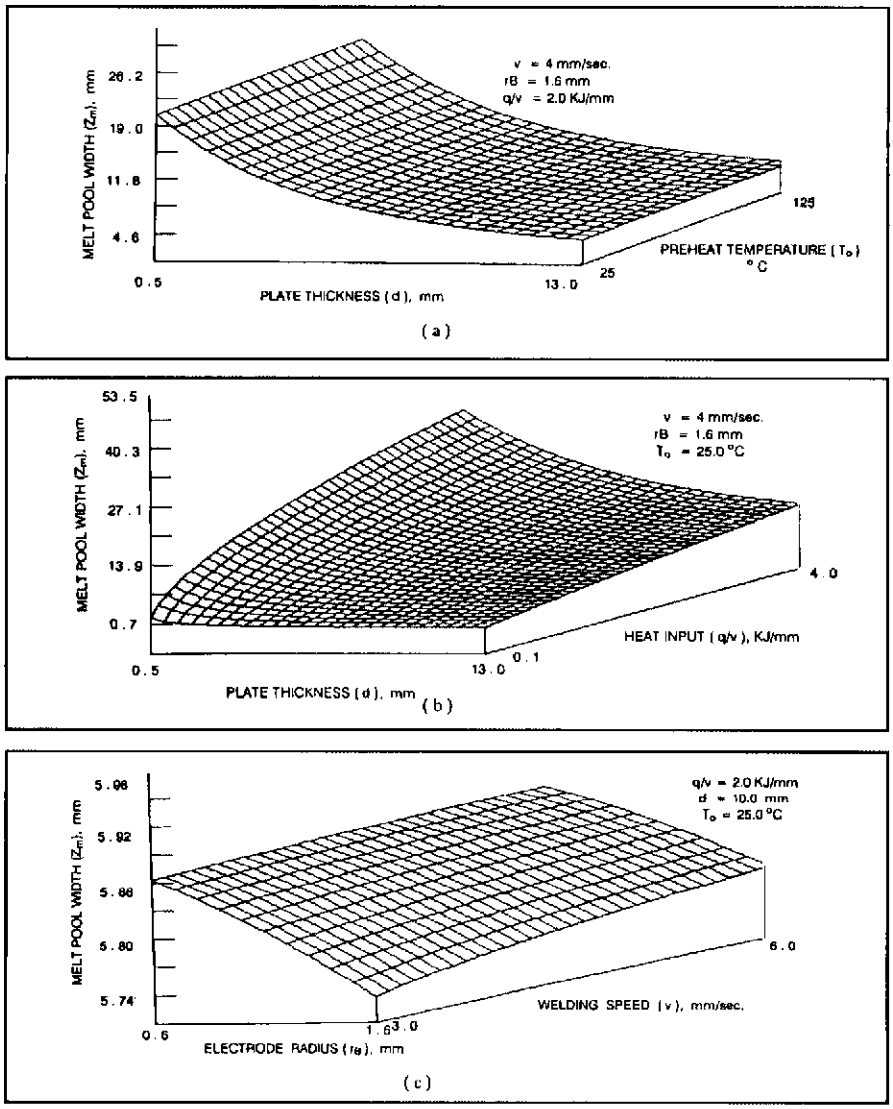

Fig. 4 — Variation of melt pool width as a function of weld variables. A — T_o and d; B — q/v and d; C — r_B and v.

It can be seen from the above equations that there are five basic variables that affect the thermal cycle. These are welding speed (v), electrode radius (r_B), preheat temperature (T_o), plate thickness (d) and the heat input (q/v). However, it can be seen from Equation 23 that the effect of these weld variables can be incorporated in the parameter, $t_{8/5}$, and the thermal cycle for a particular location, Z (*i.e.*, for a particular T_p) and a given T_o can be represented by the parameter $t_{8/5}$, Equation 25.

The parameter $t_{8/5}$ is dependent on T_o, d and effective heat input (q'/v). The effective heat input q/v is dependent on Z_0, Z_m and, hence, on v and r_B, also. Thus, the $t_{8/5}$ parameter is dependent on all the five variables. It can be inferred from the foregoing that a weld thermal cycle can be uniquely characterized by T_p, $t_{8/5}$ and T_o, as given by Equations 23–25.

It is seen from literature data (Table 1) that for most practical welding conditions for titanium the value of $t_{8/5}$ ranges from 2 to 250 s. Hence, for further evaluation of the HAZ in titanium weldments, this range of $t_{8/5}$ values is used.

Ashby and Easterling (Ref. 31) have compared the finite source solution with the results of more precise double-integral solutions and found a very good agreement between the two temperature profiles. The discrepency between the two was found to be equivalent to the experimental error involved in the studies. Hence, in this paper finite source solutions are used.

Computer Simulation

The five basic weld variables affecting the thermal cycle in the HAZ are welding speed (v), electrode radius (r_B), pre-

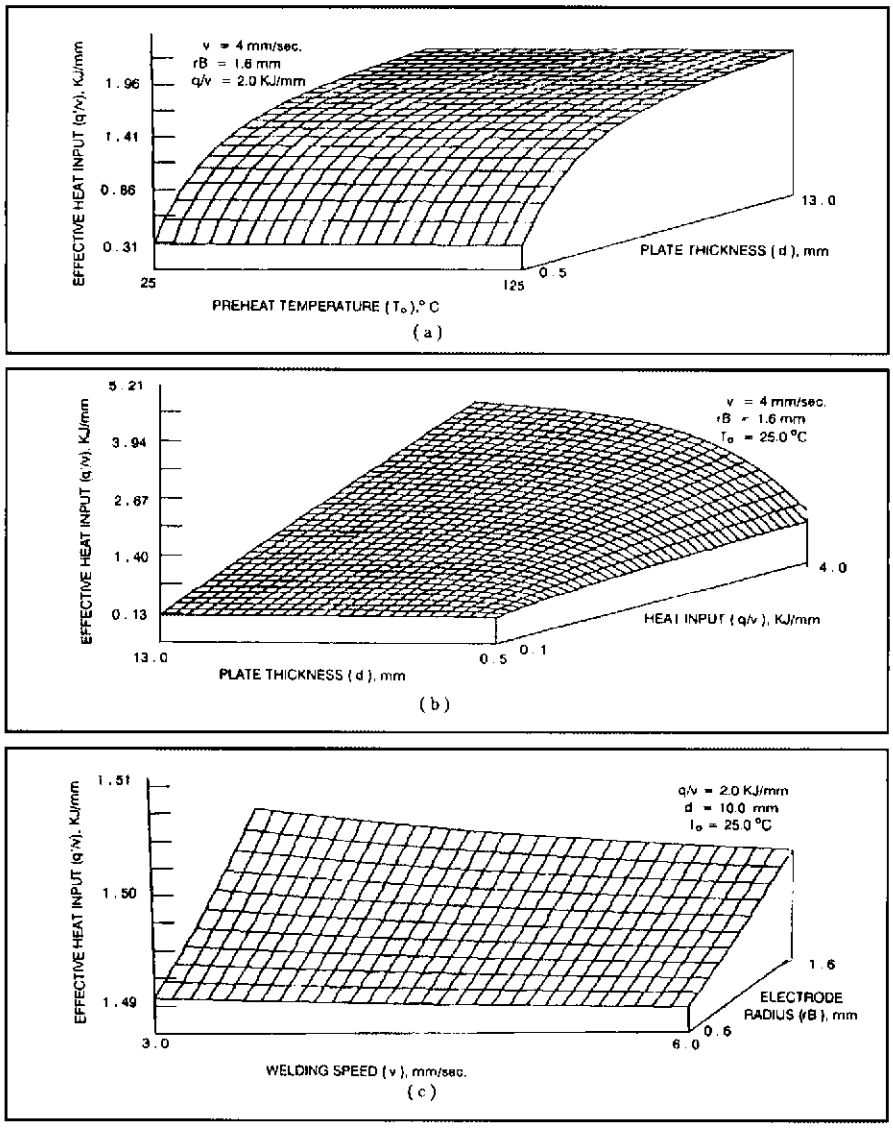

Fig. 5 — Variation of effective heat input as a function of weld variables. A — T_0 and d; B — q/v and d; C — r_B and v.

heat temperature (T_0), plate thickness (d) and heat input (q/v). The actual values of these variables used for the computer simulation studies (based on typical welding data) are listed in Table 2.

The error in the model due to variation of physical properties of the material with temperature has been offset by using the average of low- and high-temperature values. The thermal conductivity data for mill-annealed Ti-6Al-4V alloy have been reported (Ref. 35) for 293 to 923 K, which only falls in the $\alpha + \beta$ phase region. However, the data reported for CP titanium (Ref. 36) are from 500 to 1900 K, which covers the α as well as the β region. It is observed from the data of CP titanium that the thermal conductivity increases linearly with temperature during $\alpha \Rightarrow \beta$ transition and further heating in the β region. Assuming that the thermal conductivity of Ti-6Al-4V also increases linearly in the β region, the data in the high-temperature β region have been extrapolated using linear regression fit to the data in the $\alpha + \beta$ region.

Similarly, the specific heat data for Ti-6Al-4V alloy is also reported (Ref. 35) for the $\alpha + \beta$ region only. The reported data for CP titanium (Ref. 37) shows that the specific heat undergoes a sudden drop during $\alpha \Rightarrow \beta$ transition, remains constant over a small range of temperatures thereafter, and then increases with temperature in the β region. The high-temperature data is extrapolated assuming that a similar trend is followed in Ti-6Al-4V, also. For actual calculations, average values of λ and c have been used. The material properties of Ti-6Al-4V alloy used for the calculations are listed in Table 3.

The first step in the calculation is the displacement of the heat source (Z_0) by Equation 11. The melt pool width is calculated from Equation 22 by correcting the applied heat input for the arc efficiency factor. The latent heat correction is then accounted for by calculating the value of q' from Equation 21. This value of corrected heat input is used in the subsequent calculations. The parameter $t_{8/5}$ is then calculated by Equation 23. In the present study, the value of the notch factor (F_2) has been taken as 1. The peak temperature reached at different depths from the surface, and the temperature profiles at these depths for a particular value of $t_{8/5}$, are calculated from Equations 24 and 25, respectively. The flow chart for this computer program is shown in Fig. 2.

Results and Discussion

The vertical displacement of the arc, Z_0, is dependent on three welding variables, *i.e.*, v, r_B and d. Their effect on Z_0 is shown in Fig. 3. It can be seen from Fig. 3A and B that the increase in electrode diameter or the decrease in the plate thickness requires large displacement of the heat source. It is also observed that the plate thickness d has major influence and the welding speed v has minimal effect out of the three weld variables and the effect of v or r_B is significant only at lower plate thicknesses. From Fig. 3C it can be observed that the effect of r_B is an order of magnitude lower than the effect of plate thickness.

Out of the five variables considered in this study the effect of changes in the welding speed are reflected in the variation in the heat input.

Figure 4 shows the variation of the melt pool width with the variables v, r_B, d, q/v and T_0. It is observed that the melt pool width increases sharply with increase in the heat input and decrease in plate thickness. But T_0 and r_B have negligible effect and it is about an order of magnitude lower than the effect of d and q/v, Fig. 4C.

Figure 5 shows the effect of welding parameters on the effective heat input, q'/v. It can be observed that by reducing the plate thickness the effective heat input decreases sharply, Fig. 5A. This effect of d is more pronounced at higher heat inputs as compared to the effect at lower heat inputs, Fig. 5B. The other two variables, T_0 and r_B have negligible effect, which is an order of magnitude lower than the effect of q/v and d — Figs. 5A and C.

The effect of welding parameters on $t_{8/5}$ is shown in Fig. 6. It can be seen that with reducing plate thickness or increasing heat input, $t_{8/5}$ increases sharply, Figs. 6A and B. At higher heat inputs the effect of plate thickness is exponential. The pre-

heat temperature has intermediate effect, however, its effect is significant only at lower plate thickness or higher heat input, Figs. 6A and C. The electrode diameter has negligible effect on the $t_{8/5}$ parameter, Fig. 6D.

The changes in the temperature profiles at various depths, as a function of weld variables are shown in Fig. 7. It can be observed that the effect of weld variables on the temperature profiles is equivalent to their effect on the $t_{8/5}$ parameter. With increases in $t_{8/5}$ parameter, the curves become flatter and with reduction in $t_{8/5}$ the temperature curves show sharp decline during the cooling part of the weld thermal cycle.

Figures 3–7 can be extremely useful in quickly visualizing the interrelationship between the various weld variables and their effect on the thermal cycles. These figures can also be used for selection of weld variables to optimize the properties of HAZ.

Conclusions

The difficulty of a large number of weld variables affecting the weld HAZ microstructure and, thus, the properties can be overcome by using appropriate solutions to the heat flow equations to arrive at the equations defining the parameters T_p and $t_{8/5}$, which can characterize the weld thermal cycles with adequate accuracy for practical welding conditions. The heat loss due to the welding process and joint geometry can be accounted for by using the appropriate arc efficiency factor and notch factor, respectively.

The computer simulation results show that an increase in electrode diameter or decrease in plate thickness requires large displacement of the heat source above the plate surface. The melt pool width increases sharply with increase in the heat input (q/v) or decrease in plate thickness (d); however, preheat temperature (T_o) has negligible effect. The effect of weld variables on the effective heat input is also similar. The $t_{8/5}$ parameter increases sharply with reducing plate thickness or increasing heat input.

The axonometric plots can be extremely useful in quickly visualizing the interrelationship between the various weld variables and their effect on the thermal cycles, and they can also be used for selection of weld variables to optimize the properties of HAZ.

Acknowledgments

The author A. K. Shah wishes to thank Dr. P.C. Deb, Director, NCML, Bombay, for the support to carry out this research work and for his permission to publish this paper.

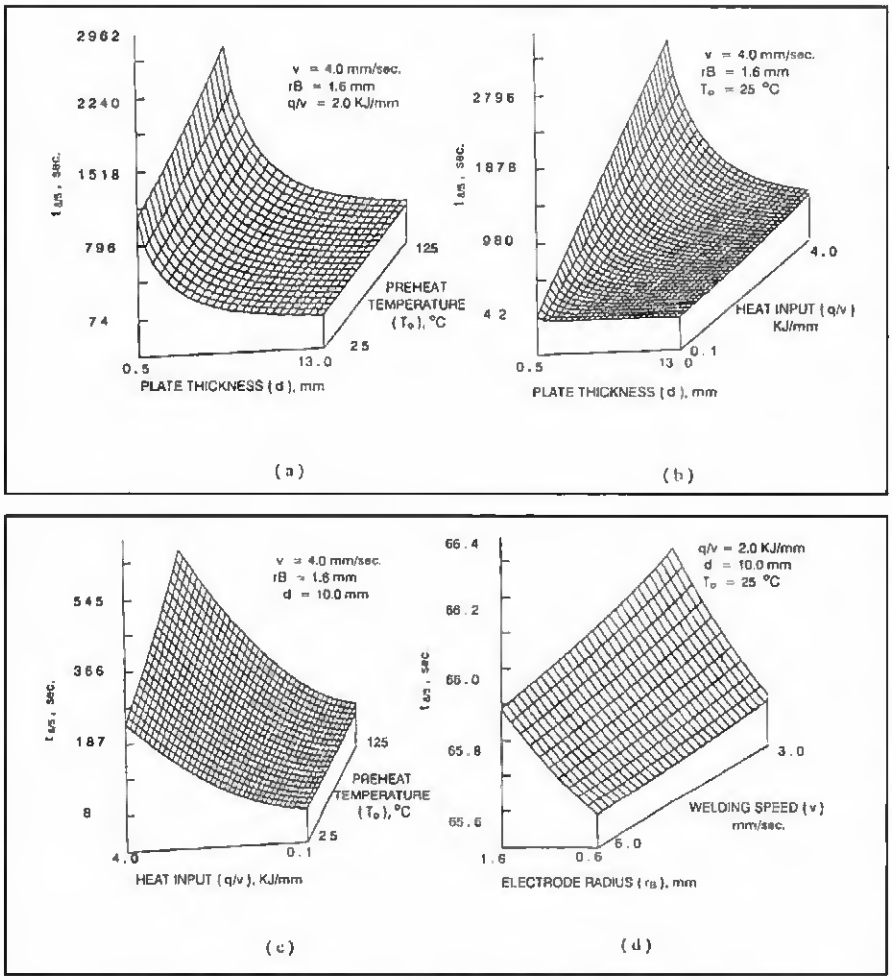

Fig. 6 — Variation of $t_{8/5}$ parameter as a function of weld variables. A — T_o and d; B — q/v and d; C — q/v and T_o; D — r_B and v.

References

1. Degenkolbe, J., Hougardy, H. P., and Uwer, D. 1980. Welding unalloyed and low alloyed structural steels. Merkblatt Stahl 381. *Beratungsstelle fur Stahlverwendung*. Dusseldorf, Germany.

2. Rosenthal, D. 1941. Mathematical theory of heat distribution during welding and cutting. *Welding Journal* 20(5): 220-s to 234-s.

3. Hess, W. F., Merrill, L. L, Nippes, E. F., and Bunk, A. P. 1943. The measurement of cooling rates associated with arc welding and their application to the selection of optimum welding conditions. *Welding Journal* 22(9): 377-s to 422-s.

4. Nippes, E. F., Merrill, L. L., and Savage, W. F. 1949. Cooling rates in arc welds in 1/2 in. plate. *Welding Journal* 28(11): 556-s to 564-s.

5. Rosenthal, D. 1946. The theory of moving sources of heat and its application to metal treatments. Trans. ASME 68: 849 866.

6. Rykalin, N.N. 1957. Calculation of heat flow during welding. *VEB Verlag Technik*, Berlin, Germany.

7. Rykalin, R. R. 1974. *Welding in the World* 12(9/10): 227 to 248.

8. Myers, P. S., Uyehara, O. A., and Borman, G. L.1967. Welding Research Council Bulletin, No.123. New York.

9. Grosh, R. J., Trabant, E. A., and Hawkins, G. A.1955. Temperature distribution in solids of variable thermal properties heated by moving heat sources. Q. *Appl. Math* 13(2): 161 to 167.

10. Jhaveri, P., Moffatt, W. G., and Adams, C. M., Jr. 1962. The effect of plate thickness and radiation on heat flow in welding anrl cutting. *Welding Journal* 41: 12-s to 16-s.

11. Swifthook, D. T., and Gick, A. E. F. 1973. Penetration welding with lasers. *Welding Journal* 52(11): 492-s to 499-s.

12. Trivedi, R., and Srinivasan, S. R. 1974. *J. Heat Transfer* 96: 427 to 428.

13. Uwer, D., and Degebkolbe, J. 1975. *Schweissen und Schneiden* 27: 303 to 306.

14. Uwer, D., and Wegmann, H. G. 1976. *Schweissen und Schneiden* 28: 132 to 136.

15. Uwer, D., and Degenkolbe, J. 1977. Characterization of the influence of welding temperature cycles on the mechanical properties of welded joints. *Stahl und Eisen* 97(24): 1201 to 1207.

16. Ghent, H., Hermance, C. E., Kerr, H. W., and Strong, A. B. 1979. *Proc. Conf. Arc*

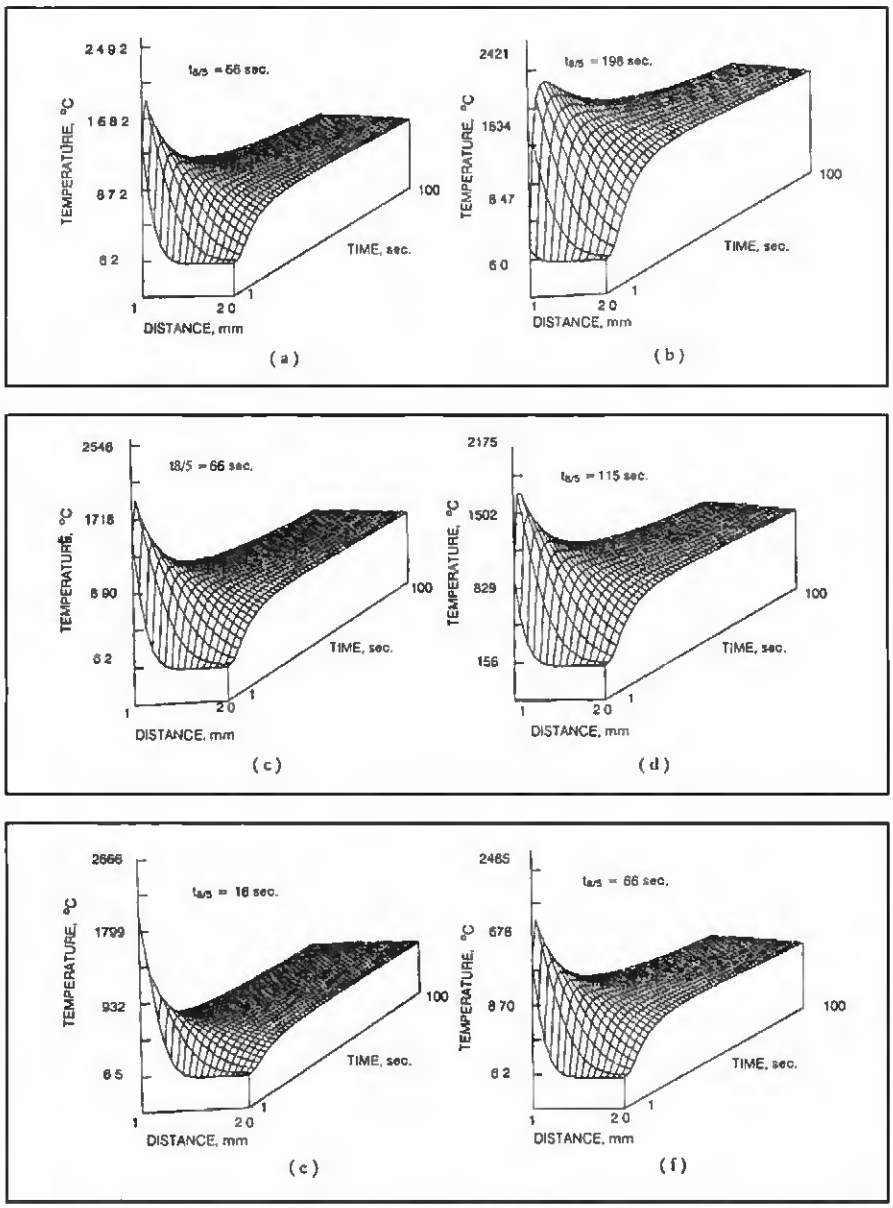

Fig. 7 — Variation of temperature profiles in the HAZ as a function of single weld variable keeping other variables constant. A — v = 4 mm/s, r_B = 1.6 mm, q/v = 2 kJ/mm, d = 10 mm and T_o = 298 K; B — d = 5 mm; C — r_B = 0.8 mm; D — T_o = 398 K; E — q/v = 1 kJ/mm; F — v = 3 mm/s

Physics and Weld Pool Behaviour, The Welding Institute, Cambridge, U.K.

17. Tsai, N. S., and Eagar, T. W. 1983. Changes in weld pool shape by variations in the distribution of heat source in arc welding. *Modelling of Casting and Welding Processes II. Proc.1983 Engineering Foundation Conferences.* pp. 317–328, The Metallurgical Society of AIME.

18. Tsai, C. L. 1983. Finite source theory. *Modelling of Casting and Welding Processes II. Proc. 1983 Engineering Foundation Conferences.* pp. 329–341, The Metallurgical Society of AIME.

19. Kou, S. 1981. Simulation of heat flow during the welding of thin plates. *Met. Trans. A* 12A(12): 2025 to 2030.

20. Goldak, J, Bibby, M., Moore, J., House, R., and Patel, B. 1986. Computer modelling of heat flow in welds. *Met.Trans. B* 17B(3): 587 to 600.

21. Uwer, D. 1987. Experience in the welding and application of high strength structural steels. *Proc. of the Int. Welding Conf.* p. 477, The Welding Research Institute and Indian Institute of Welding, New Delhi, India.

22. Easterling, K. 1983. Introduction to the physical metallurgy of welding. p. 25 *Butterworth Monographs in Metals*, Butterworth & Co. Ltd.

23. Schwenk, W, Kaehler, W. A., Jr., and Kennedy, J. R. 1967. Weldability of titanium alloy sheets 6Al-6V-2Sn and 8Al-1Mo-1V. *Welding Journal* 46(2): 64-s to 73-s.

24. Baeslack, W. A. III, Becker, D. W., and Froes, R. H. 1980. Weldability of a high toughness titanium alloy — a metallurgical evaluation. *Titanium '80: Science and Technology*, eds. H. Kimura and O. Izumi, pp. 2369–2378. The Met. Soc. of AIME.

25. Lewis, R. E., Caplan, I. L., and Coons, W. C. 1985. The elevated temperature ductility dip phenomenon in alpha, near-alpha and alpha-beta titanium alloys. *Titanium Science and Technology*, eds. G. Luetjering, U. Zwicker, and W. Bunk, pp. 895–902. Deutsche Gesellschaft fur Metallkunde e.v.

26. Hayduk, D., Damkroger, B. K., Edwards, G. R., and Olson, D. L. 1986. Cracking susceptibility of Ti-6Al-2Nb-1Ta-0.8Mo as determined by Varestraint test. *Welding Journal* 65(9): 251-s to 260-s.

27. Donachie, M. J., Jr., ed. 1988. *Titanium, a Technical Guide.* p. 141, ASM International, Materials Park, Ohio.

28. Peters, M., and Williams, J. C. 1984. Microstructure and mechanical properties of a welded (α + β)Ti alloy. Met. Trans. A 15A: 1589 to 1595.

29. Biswas, D. K., and Shah, A. K. 1984. Influence of weld variables on fracture toughness properties of weldments — some experiments with commercially pure titanium. *Proc. Sixth Int. Conf. on Fracture*, New Delhi, India.

30. Shah, A. K., Tripathi, S. M., and Biswas, D. K. 1986. Open air TIG welding of near alpha Ti-Al-Mn alloy. 40th Annual Technical Meeting of the Indian Institute of Metals, p. 79 Bombay, India.

31. Ashby, M. F., and Easterling, K. E. 1984. The transformation hardnening of steel surfaces by laser beams — I, hypoeutectoid steels. *Acta. Met.* 32(11): 1935 to 1948.

32. Bass, M. 1983. *Physical Processes in Laser-Material Interactions.* ed. M. Bertolotti, Chap. 3. New York, Plenum Press.

33. Fuerschbach, P. W., and Knorovsky. 1991. A study of melting efficiency in plasma arc and gas tungsten arc welding. *Welding Journal* 70(10): 287-s to 297-s.

34. *Metals Handbook*, Ninth Edition, Vol. 3, 1980. p 389. Ohio, ASM.

35. Touloukian, Y.S., Powell, R.W., Ho, C.Y. and Klemens, P.G. Eds.1970. Thermal Conductivity, Metallic elements & Alloys, Thermophysical properties of matter. Vol. 1., p 414. New York, Plenum Publishing Corp.

36. Touloukian, Y. S., and Buyco, E. H. eds. 1970. Specific heat, metallic elements and alloys. *Thermophysical Properties of Matter.* Vol. 4, p. 262, New York, Plenum Publishing Corp.

37. *Metals Handbook*, Tenth edition, Vol. 2, 1990, p. 1169, ASM International, Materials Park, Ohio.